Energetics of carbon peapods: Elliptical deformation of nanotubes and aggregation of encapsulated C_{60}

Susumu Okada

Center for Computational Sciences and Graduate School of Pure and Applied Sciences, University of Tsukuba, Tsukuba 305-8571, Japan and CREST, Japan Science and Technology Agency, 4-1-8 Honcho, Kawaguchi, Saitama 332-0012, Japan

(Received 28 February 2008; published 13 June 2008)

The energetics of large diameter carbon nanotubes encapsulating C_{60} molecules (peapods) have been studied by using the local density approximation in the density-functional theory (DFT). We find that the energy gain ascribed to the encapsulation of C_{60} increases under the elliptical deformation of the nanotubes compared to that for the nanotubes with circular cross section. The energy cost of the deformation of nanotubes is found to be less than 10 meV per atom and is found to be the largest for the (20,20) nanotube. We also explore the energetics of the aggregation of encapsulated C_{60} in the nanometer-scale space of the (10,10) nanotube. The total energy of the dimerized C_{60} encapsulated in the (10,10) nanotube is lower by 0.2 eV per atom than that of the isolated C_{60} indicating that the dimerization reaction is exothermic. The activation barrier for the dimerization of C_{60} is about 1.4 eV, so that the spontaneous dimerization of C_{60} is unlikely to take place without any external stimuli such as electron irradiation.

DOI: 10.1103/PhysRevB.77.235419 PACS number(s): 61.48.De, 73.22.−f

I. INTRODUCTION

Carbon nanotubes intrinsically possess a one-dimensional space on the nanometer scale within their cylindrical honeycomb network.[1] The space is applicable for application as a nanometer-scale container, which can encapsulate foreign atoms and molecules inside it.[2–5] In the early stage, lead (Pb) atoms have been encapsulated inside nanotubes with multishells (multiwalled carbon nanotubes). In addition to metal atoms, fullerenes have also been encapsulated inside single walled carbon nanotubes.[6–12] High-resolution transmission electron microscopy (HR-TEM) images clearly show the encapsulations of various fullerenes, e.g., C_{60}, C_{70}, C_{80}, and C_{84}, as well as metallofullerenes, e.g., $Gd@C_{82}$ and $Sc_2@C_{84}$ inside single-walled nanotubes. These unusual structures occasionally called carbon peapods, can be classified as a new class of crystalline carbon with novel structural hierarchy: The structure of the peapods is characterized by an interesting combination of one- and zero-dimensional constituent units, i.e., carbon nanotubes and fullerenes. In this hierarchical solid, the electronic structure is found to depend on the electronic structure of each constituent and on the space between them.[13–15] For instance, the fundamental energy gap of peapods consisting of semiconducting nanotubes changes in a range from moderate gap semiconductors to metals by varying the type of encapsulated fullerene species.[15]

In our previous researches, it was also found that the space between encapsulated fullerenes and nanotubes plays a crucial role in determining their energetics. For the C_{60}, it was demonstrated that a nanotube with diameter of 13.5 Å possesses the largest energy gain following the encapsulation of these molecules. In this case, the nanotube provides a favorable space for C_{60} encapsulation, in which the C_{60} are tightly bound with the interwalls having spacings of about 3.3 Å. For the structure, if we assume that C_{60} are placed on the nanotube axis, the binding energy of C_{60} monotonically decreases and gradually approaches zero by increasing the diameter of the nanotubes.[14,15] In the case of peapods consisting of large diameter nanotubes, however, the calculated situation is not realistic. The transmission electron microscopy experiment clearly show that the C_{60} molecules are located at the vicinity of the nanotube walls.[16] Moreover, the large diameter nanotubes are usually squashed along the radial direction, resulting in the elliptical cross section following encapsulation of C_{60}.[16]

Besides, with the structural modification of nanotubes, in the early experiments, it has been demonstrated that C_{60} also change its structure under electron-beam irradiation in the HR-TEM experiment.[6–9] Encapsulated C_{60} are occasionally found to be irregularly aligned in nanotubes and are sometimes found to be polymerized by forming covalent bonds between adjacent molecules. Further irradiation results in the coalescence of C_{60} forming tubular structures inside the nanotubes.

The experiments have directly provided structural information about carbon nanopeapods, such as the deformation of nanotubes and the coalescence of C_{60}. However, quantitative discussions on such structural modifications to the nanotubes and encapsulated fullerene molecules have not been addressed as yet. Thus, the purposes of this work are to unravel the energetics and electronic structures of carbon nanopeapods in terms of the structural modifications to the wall of the nanotubes and the coalescence of the C_{60} encapsulated in the nanotubes. Our first-principles total-energy calculations provide the energetics of C_{60} encapsulated within nanotubes with structural deformation. The formation energies of peapods with deformed nanotubes possessing elliptical cross sections are larger than those with cylindrical nanotubes indicating the fact that C_{60} molecules are more tightly bound inside the deformed nanotubes. The cross sections of the nanotubes encapsulating C_{60} are determined by the competition between the energy cost of the deformation of nanotubes and the energy gain afforded by the C_{60} encapsulation. We also explore the energetics associated with the aggregation of encapsulated C_{60} inside the nanometer-scale space of the

(10,10) nanotube. It is found that the dimerization of C_{60} inside the nanotube is exothermic. However, the activation barrier for the dimerization is found to be 1.4 eV, indicating that the polymerization is unlikely to take place without any high-energy processes such as electron irradiation and photon irradiation.

The manuscript is organized as follows. In Sec. II, we explain the computational procedures used in the electronic-structure calculation. Results and discussion are given in Sec. III. Section IV summarizes and concludes the paper.

II. COMPUTATIONAL METHODS

In the present work, we use the PSPW code[17] to study the energetics and electronic structure of the systems. All calculations have been performed by density-functional theory (DFT).[18,19] The exchange-correlation energy of interacting electrons is treated in the local density approximation (LDA) with a functional form fitted to the Ceperley–Alder result.[20–22] Norm-conserving pseudopotentials generated by using the Troullier–Martins scheme are adopted to describe the electron-ion interaction.[24,25] The valence wave functions are expanded by the plane-wave basis set with a cutoff energy of 50 Ry (680.25 eV), which gives enough convergence of the relative total energies of carbon-related materials.[13] We have adopted a supercell model in which a nanotube is placed with its wall positioned 6 Å away from the outer wall of an adjacent nanotube. Along the tube direction, we have imposed a commensurability condition between the one-dimensional periodicity of the atomic arrangements in the nanotube and that of the chain of C_{60}. Consequently, the lattice parameter c becomes 9.824 Å along the tube direction, which corresponds to the quadruple of the periodicity of armchair nanotubes. In addition, we have also considered a lattice parameter that is eightfold that of the periodicity of armchair nanotubes ($c=19.648$ Å) in order to explore the possibility of long-range modulation and the aggregation of C_{60}. Integration over the one-dimensional Brillouin zone is carried out using the two k points. We have also used the conjugate-gradient minimization scheme both for the electronic-structure calculation and for the geometry optimization.[17] The structural optimization has been performed until the remaining forces for each atom are less than 5 mRy/Å (68 meV/Å) under the above lattice parameters. We have also used the constraint minimization scheme to evaluate the activation barriers for the coalescence of C_{60} inside the nanotubes.[26]

In the present study, we carried out calculations for carbon peapods consisting of C_{60} and armchair (n,n) nanotubes using $n=12\sim20$ with circular and elliptically deformed cross sections to elucidate the energetics of the nanotube deformations. For the aggregation of the encapsulated C_{60}, we performed calculations for peapods consisting of C_{60} and (10,10) nanotubes.

III. RESULTS AND DISCUSSION

A. Energetics of peapods

Figure 1 shows the optimized geometries of peapods with elliptically deformed and circular cross sections for various tube circumference lengths. In the deformed nanotubes, we consider that these comprise nanotubes with elliptical cross sections consisting of half pipes of (10,10) nanotubes and graphene ribbons with appropriate width inserted into the two half pipes. It should be noted that a variety of squashed deformation of nanotubes is likely to take place in experiments. However, in the present work, we focus on the above structure to evaluate the upper limit of the energetics of peapods with deformed nanotubes. Our total-energy calculations clearly show that the optimum position of the C_{60} in these large diameter nanotubes with circular and deformed cross sections is dislodged from the center of the nanotube: The C_{60} are located 6.5 Å from the wall of the nanotube to keep a preferable interwall distance of about 3.3 Å irrespective of the nanotube diameters and cross sections.

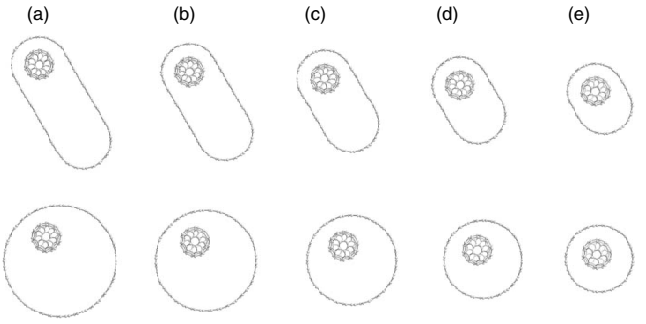

FIG. 1. Optimized geometries of peapods having walls that consist of (a) (20,20), (b) (18,18), (c) (16,16), (d) (14,14), and (e) (12,12) nanotubes. In each figure, upper and lower structures correspond to nanotubes with the same circumference lengths in elliptical and circular cross sections, respectively.

We also explore the stability of the C_{60} peapods with various tube radii possessing circular and elliptical cross sections. The stability is evaluated by calculating the energy difference in the following reaction:

$$(n,n)\text{tube} + C_{60} \rightarrow C_{60} @ (n,n) - \Delta E.$$

Figure 2 shows the energy ΔE of the C_{60} peapods as a function of the circumference length of the nanotubes. The encapsulation of C_{60} within the deformed nanotubes is more favorable than for the circular nanotubes with the same circumference lengths. It is found that the energy gain associated with the encapsulation for the deformed nanotubes is 1 eV per C_{60} irrespective of the tube circumference. This property is ascribed to the fact that the local atomic configuration of the deformed nanotubes surrounding the C_{60} is common for all tube circumferences: C_{60} are surrounded by the half pipe of the (10,10) nanotube and two parallel graphene sheets separated by 13.5 Å giving the exact preferable spacing for the intercalation of C_{60} molecules, as in the case of C_{60}-graphite cointercalation compounds.[27]

In sharp contrast to the deformed nanotubes, by increasing the nanotube radii, the energy gain associated with the encapsulation for the circular nanotubes gradually approaches about 0.2 eV, which corresponds to the energy gain of adsorption of C_{60} on the graphene monolayer. In these cases, the contact area between the nanotubes and C_{60} monotonically decreases with increasing tube diameter. Thus, the

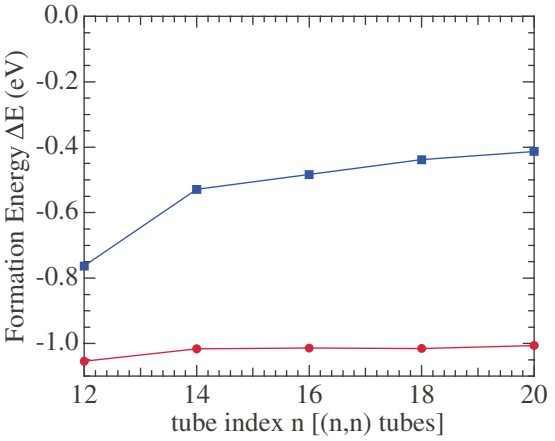

FIG. 2. (Color online) Reaction energies ΔE (see text) per C_{60} in the encapsulation reaction for the (12,12), (14,14), (16,16), (18,18), and (20,20) armchair nanotubes with circular (blue squares) and elliptical (red circles) cross sections.

results indicate that the encapsulation of C_{60} enhances the deformation of large diameter nanotubes substantially. Furthermore, once C_{60} are encapsulated into the deformed nanotubes, they are more tightly bound inside and are unlikely to be released from the inner space of the nanotubes. By modifying the cross sections of the large diameter nanotubes, the resulting nanotubes would be applicable for use as nanomaterial-delivery systems. Indeed, a recent translation microscopy experiment clearly shows the structural deformation of large diameter nanotubes encapsulating C_{60}, and the encapsulated C_{60} have been found to be more tightly bound inside the deformed nanotubes than within the circular nanotubes.[16]

It is expected that the energy gain ΔE depends on the C_{60} position in the nanotubes. Figure 3 shows ΔE as a function of the C_{60} position in the deformed and circular (12,12) nanotubes. It is found that the energy ΔE of the nanotube with deformed shape is always lower than that of the circular nanotube. This larger encapsulation energy ($|\Delta E|$) for the deformed nanotube is ascribed to the geometric structure around the C_{60}: The C_{60} are sandwiched between two graphene sheets with favorable graphene-C_{60} distances of about 3.3 Å in the deformed nanotubes.

Although, the center of the nanotubes is the saddle point of the energy ΔE for both circular and elliptical nanotubes. For the deformed nanotubes with sufficient thickness, the ΔE has a plateau around the center of the nanotubes, at which ΔE has a value of about 0.4 eV corresponding to a value double that of the binding energy of C_{60} on the graphene monolayer [Fig. 3(b)]. In sharp contrast, in the circular nanotubes, the interaction between C_{60} and the nanotube monotonically decreases when the C_{60} approaches the center of the nanotubes so that ΔE is zero for very large diameter nanotubes [Fig. 3(a)]. The energetics results in the different packing structures of C_{60} inside the large diameter nanotubes depending on the cross sections of the nanotubes. For the circular nanotubes, C_{60} are basically packed in a helical arrangement in which the C_{60} locally form a two-dimensional triangular lattice along the wall of the nanotubes.[28,29] In sharp contrast, in the deformed nanotubes, the C_{60} form one-

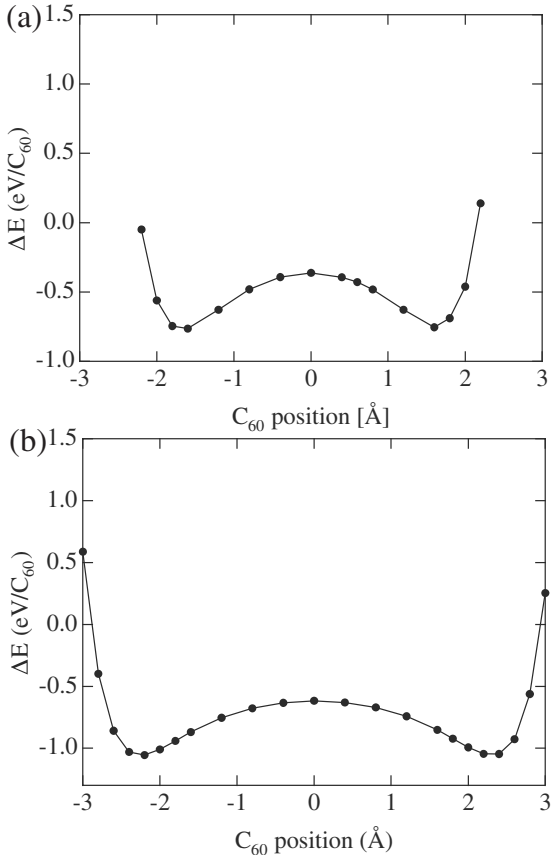

FIG. 3. Total energies of C_{60}@(12,12) peapods per unit cell for the various radial positions of the C_{60} in the (12,12) nanotube with (a) circular and (b) deformed cross sections. The energies are measured from those of the C_{60}@(12,12), in which the C_{60}'s are located at the center of the nanotube.

dimensional arrays located at both sides of the nanotubes under low C_{60} concentrations and a layered arrangement under high C_{60} concentrations. Thus, the confined C_{60} inside the deformed nanotubes may realize new one-and two-dimensional sciences based on the C_{60}.

B. Energetics of nanotubes

To provide a quantitative discussion on the deformation of nanotubes following C_{60} encapsulation, we studied the energetics of deformation of empty nanotubes. It is well known that the total energy of nanotubes is inversely proportional to the square of their radii and asymptotically approaches the total energy of the monolayer graphite. Figure 4(a) shows the total energy of the circular nanotubes and deformed nanotubes consisting of half pipes of (10,10) nanotubes and two graphene sheets connecting the half pipes.

The asymptotic behavior of the total energy of the deformed nanotubes exhibits different characteristics to that of the circular nanotubes. The total energy of the deformed nanotubes approaches zero more slowly compared to that for the circular nanotubes. In this case, the total energy is inversely proportional to the radius of the nanotubes. The energy differences between the circular and deformed nano-

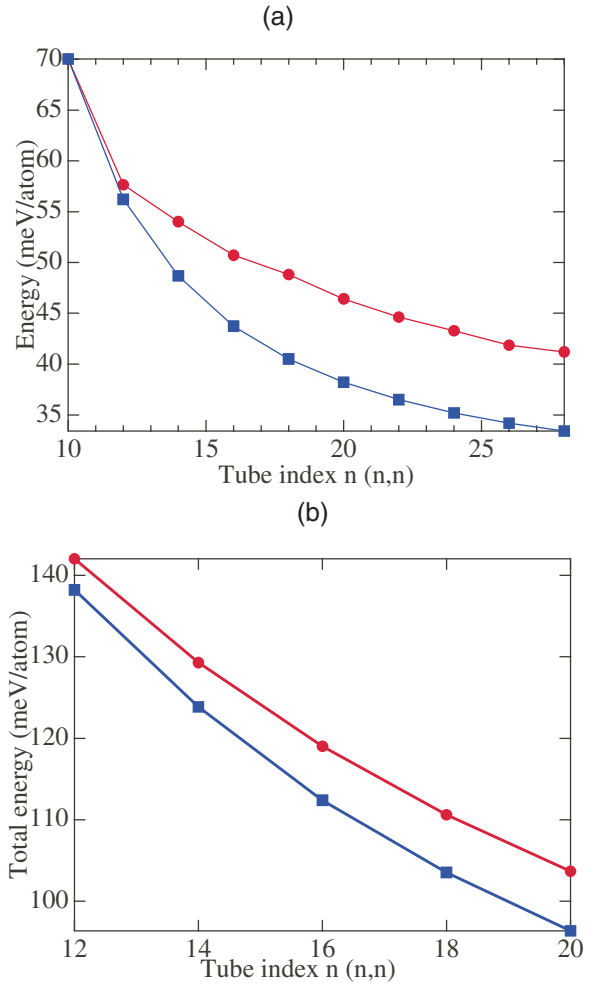

FIG. 4. (Color online) Total energies of (a) empty and (b) C_{60}-filled carbon nanotubes as a function of nanotube circumference length. In each panel, the red circles and blue squares denote the nanotubes with circular and elliptically deformed cross sections, respectively. The energies are measured from that of the graphite monolayer.

tubes with the same circumference length are found to be less than a few millielectron volt per atom.[30] This difference has a maximum for the (20,20) nanotubes and gradually decreases by increasing the tube diameter or circumference length [Fig. 4(a)]. Thus, for the peapods studied here, the total energy of the peapods consisting of deformed nanotubes is higher than that for peapods consisting of circular nanotubes, even though the large energy gain associated with C_{60} encapsulation is expected to take place [Fig. 4(b)]. However, for the peapods consisting of thicker nanotubes or more densely packed with C_{60}, the deformed nanotubes incorporating the C_{60} are likely to be the ground-state structure of the peapod. Indeed, the HR-TEM study shows the thicker peapods consist of nanotubes with a squashed shape. The results indicate that the cross section of the large diameter nanotubes are determined by the competition between the energy cost associated with the deformation of the nanotubes and energy gain brought about by the C_{60} encapsulation.

TABLE I. The energy level of the bottom of the t_{1u} state and its bandwidth of C_{60} encapsulated in the (12,12) nanotube for various C_{60} positions. The energies are measured from the point at which the π and π^* bands of the (12,12) nanotube cross each other. Calculated values are obtained at the distance between the wall of the nanotube and the encapsulated C_{60}, d=2.4, 3.3, 4.4, and 6.0 Å.

Distance	2.4	3.3	4.4	6.0
Level energy (eV)	0.42	−0.02	0.08	−0.05
Band width (eV)		0.23	0.39	0.22

C. Electronic structures of peapods

Table I shows the energy level of the bottom of the t_{1u} state and its bandwidth of C_{60} encapsulated within the (12,12) nanotube for various C_{60} positions. As shown in Table I, it is found that the energy level of the t_{1u} states strongly depends on the C_{60} position inside the nanotube. The t_{1u} states shift significantly upward when the C_{60} is located 5.9 Å from the wall of the nanotubes, in which the interwall distance is 2.4 Å. By increasing the interwall distance, the t_{1u} states gradually shift downward then cross the Fermi level resulting in multicarrier metals in which the electrons and holes exist on C_{60} and on the nanotube, respectively. The largest shift does not occur at the interwall distance of about 3.3 Å corresponding to the most energetically stable C_{60} position but at a slightly larger interwall distance. Further separation of C_{60} results in an upward shift of the t_{1u} states.

In addition to the t_{1u} energy, the width of the t_{1u} states also exhibits the same characteristics. The width is at its maximum when it is larger than the optimum distance between the walls of the C_{60} and the nanotube. Thus, the results indicate that the hybridization between the electron states of the C_{60} and of the nanotube is the largest for the intercell distance slightly larger than the distance of 3.3 Å, which is the most energetically stable position of the C_{60} inside the nanotubes.

D. Dimerization of C_{60}

Many HR-TEM experiments have shown that encapsulated C_{60} tend to gather together resulting in the long-range modulation of the inter-C_{60} distance inside the nanotubes.[6–9] Here, we explore the possibility of the long-range modulation with double periodicity of C_{60} inside the (10,10) nanotube. The t_{1u} states are partially occupied by electrons transferred from the nanotube, and the C_{60} are weakly bound to each other by a weak intermolecular interaction.[13] These facts are expected to induce the modulation of the alignment of C_{60} in the nanotubes. However, such modulation with double periodicity does not take place in the system. As shown in Fig. 5, we do not find any minima in the total energy of the peapod as a function of the inter-C_{60} distance. The total energy monotonically increases as the inter-C_{60} distance is decreased. However, for modulations longer than the triple periodicity, these modulations avoid the partial occupation of the t_{1u} band, which is still expected to take place.

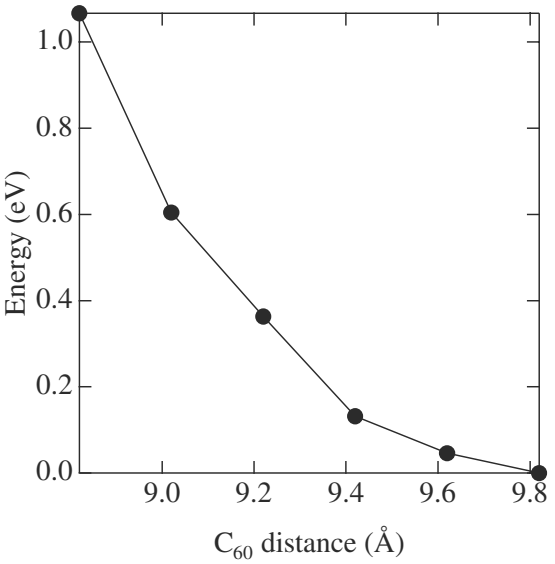

FIG. 5. Total energy of the C_{60} encapsulated within the (10,10) nanotube as a function of the intermolecular distance. The energy is measured from that obtained in the C_{60} arrangement when the C_{60} are equidistantly aligned at x=9.824 Å [E2].

Besides the nonequidistance arrangements of C_{60}, it has also been observed that C_{60} forms covalent bonds with its adjacent molecules and transforms into tubular fullerenes under electron-beam irradiation during the HR-TEM experiments.[7–9] The results indicate that the polymerization of C_{60} takes place inside the nanotubes. It is well known that high pressure treatment under elevated temperature[31–33] and photoirradiation[34,35] for the solid C_{60} results in the formation of polymeric phases of C_{60}. Here, we have explored how nanotubes affect the energetics of C_{60} polymerization. Figure 6 shows the optimized structure of dimerized C_{60} encapsulated within a (10,10) nanotube. In the structure, dimerization is attained via the formation of a four-membered ring associated with two 66 bonds (double bond), each of which is shared by the two hexagons. The calculated bond length connecting the adjacent molecules is 1.5 Å, which is

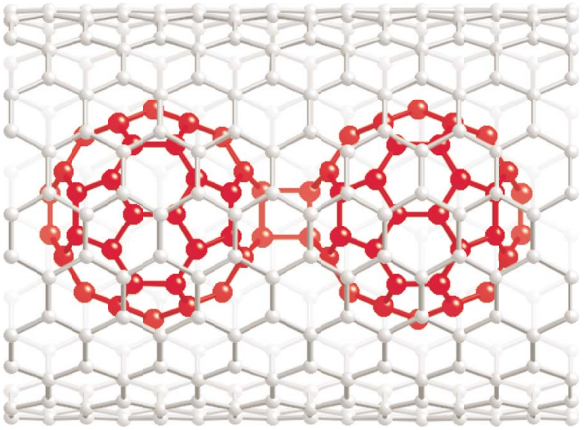

FIG. 6. (Color online) Optimized structures of dimerized C_{60} encapsulated within the (10,10) nanotube. Red and gray circles denote the atoms belonging to the C_{60} dimer and the nanotube, respectively.

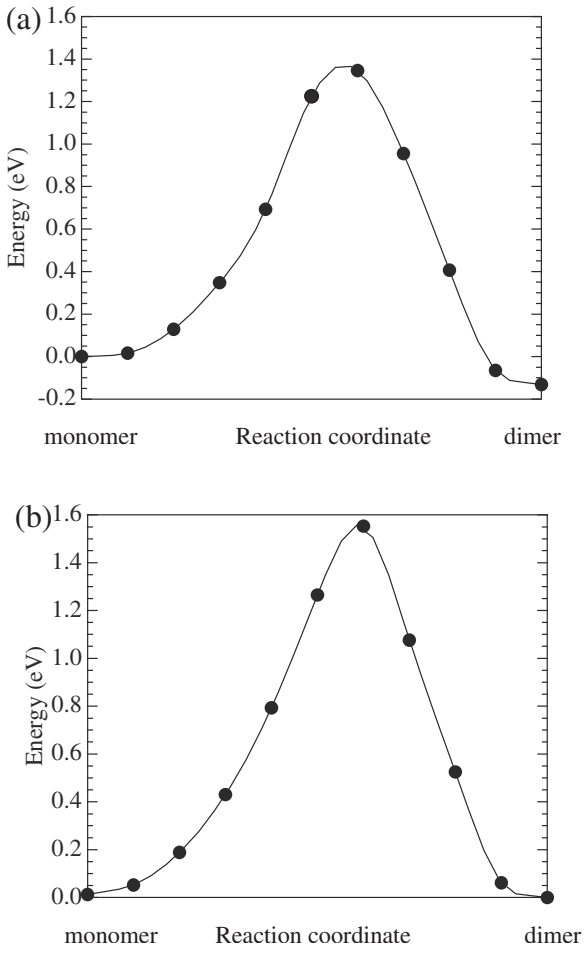

FIG. 7. Total energies of the C_{60} (a) encapsulated within the (10,10) nanotube and (b) unwrapped as a function of the intermolecular distance. The energy is measured from that obtained from the equidistance C_{60} arrangement. The lines are provided as a visual guide.

the same as that in the isolated C_{60} dimers. Further analysis on the charge-density distribution corroborates that the atoms involved in the dimerization are in sp^3-like hybridization.[36,37]

In Fig. 7, we show the total energies of the C_{60} encapsulated within the nanotube before and after dimerization, as well as the total energies for the isolated case. In addition, based on the constraint minimization scheme, we also show the total energies of the system as a function of the distance between adjacent molecules, which corresponds to the reaction coordinates of the dimerization. From Fig. 7, we can roughly estimate the activation barrier for the dimerization of C_{60}, which corresponds to a saddle point geometry between the isolated and dimerized C_{60}. The activation barrier is found to be 1.4 eV per C_{60}, indicating that polymerization is unlikely to occur without the influence of a high-energy process such as high pressure, electron-beam irradiation, or photon irradiation. A recent ^{13}C-NMR experiment confirms the fact that the C atoms of the encapsulated C_{60} are in the sp^2 hybridization state indicating the absence of intermolecular covalent bonds prior to electron-beam irradiation.[38]

Although, the spontaneous polymerization of C_{60} is unlikely to take place inside the nanotubes, the wall of the

nanotubes decreases the activation barrier of the dimerization by some 0.2 eV more than that for the unwrapped C_{60}'s. Furthermore, the total energy of the dimerized C_{60} encapsulated within the nanotube is lower by some 0.2 eV more than that for the isolated C_{60} in the equidistance arrangement. Thus, the polymerization of C_{60} inside the nanotubes is found to be an exothermic reaction. In sharp contrast, in the unwrapped C_{60} chain, the total energy of the dimerized phase is almost the same as that for the isolated arrangement.

IV. SUMMARY

Here, we have studied the energetics of nanotubes encapsulating C_{60} in terms of both the structural deformation of the nanotubes and the aggregation of encapsulated C_{60}, based on first-principles total-energy calculations. The formation energies of peapods with deformed nanotubes possessing an elliptical cross section are found to be larger than those for the cylindrical nanotubes indicating the fact that the C_{60} molecules are more tightly bound inside the deformed nanotubes. Furthermore, the energy gain associated with the encapsulation in the deformed nanotubes is about 1 eV irrespective of the tube circumference length, since the local geometries of the deformed nanotubes wrapped around the C_{60} are common for the nanotubes studied. On the other hand, based on the calculations of the empty nanotubes, we clarified that the energy cost for the deformation of the nanotubes from circular to elliptical cross sections is less than 10 meV per atom. Thus, we conclude that the cross section of the nanotubes encapsulating C_{60} is determined by the competition between the energy cost of the deformation of nanotubes and the energy gain of the C_{60} encapsulation. Our findings can excellently explain the experiment in which the deformation of the large diameter nanotubes encapsulating C_{60} is clearly observed.

We also explored the energetics of encapsulated C_{60} to give a theoretical insight into the aggregation of C_{60} within the nanotubes under TEM observation. It was found that the dimerization reaction of C_{60} inside the nanotube is exothermic. The dimerization of C_{60} decreases the total energy by 0.1 eV per C_{60}. However, the activation barrier for the dimerization is found to be 1.4 eV indicating that polymerization is unlikely to take place without the influence of high-energy processes such as electron irradiation and photon irradiation. The results infer that the experimentally observed polymerization or aggregation of C_{60} is induced by the electrons supplied during the TEM observation. On the other hand, unlike free C_{60}, those C_{60} encapsulated within nanotubes undergo aggregation as promoted by the nanotubes.

ACKNOWLEDGMENTS

We would like to thank A. Oshiyama for providing the DFT program used in this work. We also thank Y. Maniwa for communicating his results prior to publication. This work was partly supported by CREST-JST, Japan Science and Technology Agency, and a grant-in-aid for scientific research from the Ministry of Education, Culture, Sports, Science and Technology of Japan. Computations were performed on an NEC SX-8/4B at the Center for Computational Sciences, University of Tsukuba, an NEC SX-8 at the Yukawa Institute of Theoretical Physics, Kyoto University, an NEC SX-8R at the Cybermedia Center, Osaka University, an NEC SX-7 at the Information Synergy Center, Tohoku University, and an NEC SX-7 at the Research Center of Computational Science, Okazaki National Institute.

[1] S. Iijima, Nature (London) **354**, 56 (1991).
[2] P. M. Ajayan and S. Iijima, Nature (London) **361**, 333 (1993).
[3] R. S. Lee, H. J. Kim, J. E. Fisher, A. Thess, and R. E. Smalley, Nature (London) **388**, 854 (1997).
[4] C. Bower, S. Suzuki, K. Tanigaki, and O. Zhou, Appl. Phys. A: Mater. Sci. Process. **67**, 47 (1998).
[5] C. Bower, A. Kleinhammes, Y. Wu, and O. Zhou, Chem. Phys. Lett. **288**, 481 (1998).
[6] B. W. Smith, M. Monthioux, and D. E. Luzzi, Nature (London) **396**, 323 (1998).
[7] B. Burteaux, A. Claye, B. W. Smith, M. Monthioux, D. E. Luzzi, and J. E. Fischer, Chem. Phys. Lett. **310**, 21 (1999).
[8] B. W. Smith, M. Monthioux, and D. E. Luzzi, Chem. Phys. Lett. **315**, 31 (1999).
[9] J. Sloan, R. E. Dunin-Borkowskib, J. L. Hutchisonb, K. S. Colemana, V. C. Williamsa, J. B. Claridgea, A. P. E. Yorka, C. Xua, S. R. Baileya, G. Browna, S. Friedrichsa, and M. L. H. Green, Chem. Phys. Lett. **316**, 191 (2000).
[10] H. Kataura, Y. Kumazawa, Y. Maniwa, I. Umezu, S. Suzuki, Y. Ohtsuka, and Y. Achiba, Synth. Met. **121**, 1195 (2001).
[11] K. Hirahara, S. Bandow, K. Suenaga, H. Kato, T. Okazaki, H. Shinohara, and S. Iijima, Phys. Rev. B **64**, 115420 (2001).
[12] K. Hirahara, K. Suenaga, S. Bandow, H. Kato, T. Okazaki, H. Shinohara, and S. Iijima, Phys. Rev. Lett. **85**, 5384 (2000).
[13] S. Okada, S. Saito, and A. Oshiyama, Phys. Rev. Lett. **86**, 3835 (2001).
[14] S. Okada, M. Otani, and A. Oshiyama, Phys. Rev. B **67**, 205411 (2003).
[15] M. Otani, S. Okada, and A. Oshiyama, Phys. Rev. B **68**, 125424 (2003).
[16] J. Fan, M. Yudasaka, R. Yuge, D. N. Futaba, K. Hata, and S. Iijima, Carbon **45**, 722 (2007).
[17] O. Sugino and A. Oshiyama, Phys. Rev. Lett. **68**, 1858 (1992).
[18] P. Hohenberg and W. Kohn, Phys. Rev. **136**, B864 (1964).
[19] W. Kohn and L. J. Sham, Phys. Rev. **140**, A1133 (1965).
[20] J. P. Perdew and A. Zunger, Phys. Rev. B **23**, 5048 (1981).
[21] D. M. Ceperley and B. J. Alder, Phys. Rev. Lett. **45**, 566 (1980).
[22] Since LDA is known to overestimate the binding energy between graphitic materials (Ref. 23), the encapsulation energies shown here are slightly larger than those evaluated in the experiments.
[23] L. A. Girifalco and M. Hodak, Phys. Rev. B **65**, 125404 (2002).
[24] N. Troullier and J. L. Martins, Phys. Rev. B **43**, 1993 (1991).
[25] L. Kleinman and D. M. Bylander, Phys. Rev. Lett. **48**, 1425 (1982).

[26] A. Ulitsky and R. Elber, J. Phys. Chem. **92**, 1510 (1990).
[27] S. Saito and A. Oshiyama, Phys. Rev. B **49**, 17413 (1994).
[28] A. N. Khlobystov, D. A. Britz, A. Ardavan, and G. A. D. Briggs, Phys. Rev. Lett. **92**, 245507 (2004).
[29] K. S. Troche, V. R. Colucl, S. F. Braga, D. D. Chinellato, F. Sato, S. B. Legosa, R. Rurali, and D. S. Galvao, Nano Lett. **5**, 349 (2005).
[30] S. B. Fagan, L. B. da Silva, and R. Mota, Nano Lett. **3**, 289 (2003).
[31] Y. Iwasa, T. Arima, R. M. Fleming, T. Siegrist, O. Zhou, R. C. Haddon, L. J. Rothberg, K. B. Lyons, H. L. Carter, Jr., A. F. Hebard, R. Tycko, G. Debbagh, J. J. Krajewski, G. A. Thomas, and T. Yagi, Science **264**, 1570 (1994).
[32] M. Núñez-Regueiro, L. Marques, J.-L. Hodeau, O. Béthoux, and M. Perroux, Phys. Rev. Lett. **74**, 278 (1995).
[33] G. Oszlanyi and L. Forro, Solid State Commun. **93**, 291 (1995).
[34] A. M. Rao, P. Zhou, K. Wang, G. T. Hager, J. M. Holden, Y. Wang, W. Lee, X. Bi, P. C. Eklund, D. S. Cornett, M. A. Duncan, and I. J. Amster, Science **259**, 955 (1993).
[35] O. Chauvet, G. Oszlanyi, L. Forro, P. W. Stephens, M. Tegze, G. Faigel, and A. Janossy, Phys. Rev. Lett. **72**, 2721 (1994).
[36] S. Okada and S. Saito, Phys. Rev. B **55**, 4039 (1997).
[37] S. Okada and S. Saito, Phys. Rev. B **59**, 1930 (1999).
[38] K. Matsuda, Y. Maniwa, and H. Kataura, Phys. Rev. B **77**, 075421 (2008).